Aerosol and Air Quality Research

Assessment of the Contribution of Local and Regional Biomass Burning on PM$_{2.5}$ in New York/New Jersey Metropolitan Area

Subraham Singh[1], Glen Johnson[1], David W. DuBois[2], Ilias G. Kavouras [1*]

[1] Department of Environmental, Occupational and Geospatial Health Sciences, City University of New York Graduate School of Public Health and Health Policy, New York, NY, USA
[2] Department of Plant and Environmental Sciences, New Mexico State University, Las Cruces, NM, USA

ABSTRACT

The sources of fine particulate matter (PM$_{2.5}$, particles with diameter < 2.5 μm) in four monitoring sites in the New York/New Jersey metropolitan statistical area from 2007 to 2017 were apportioned by positive matrix factorization (PMF) of chemical speciation data. Biomass burning, secondary inorganic (i.e., ammonium sulfate and nitrate) and primary traffic exhausts were the predominant PM$_{2.5}$ sources. The declining trends of PM$_{2.5}$ mass in all four sites were very well correlated with decreasing secondary sulfate levels due to SO$_2$ emission reductions by coal-fired power plants. The contributions of secondary nitrate, primary traffic exhausts and diesel particles did not change (or slightly increased) over time except for the Queens site, where statistically significant declines were computed. Biomass burning contributions increased in the Queens and Chester sites but declined in the Division Str and Elizabeth Lab sites, although significant interannual variability was observed. Wintertime biomass burning aerosols were most likely due to combustion of contemporary biomass for industrial and domestic heating, and it was linked to the intensity (average minimum temperature) and duration (number of freezing days) of cold weather. The annual summertime biomass burning contributions were correlated with the number of and area burnt by lightning-ignited wildfires. These results indicate that PM$_{2.5}$ sources in urban environments is changing from anthropogenic secondary sulfate and nitrate to carbonaceous aerosol from local anthropogenic and regional climate-driven biomass burning. This trend may counterbalance emissions controls on anthropogenic activities and modify the biological and toxicological responses and resultant health effects.

Keywords: Fine aerosol, Sources, Wildfires, Woodburning, Traffic

1 INTRODUCTION

Atmospheric particulate matter changes the earth's energy budget directly through scattering or absorption of the solar and infrared radiation and indirectly through modification of the thermal diffusion parameters of cloud condensation nuclei (Shikwambana *et al.*, 2020). Inhalation of atmospheric aerosol is linked to onset of cardiovascular and cerebrovascular diseases (Rajagopalan *et al.*, 2018) including myocardial infarctions (Evans *et al.*, 2017), ischemic stroke (Shah *et al.*, 2015), and cardia arrythmia (Link *et al.*, 2013), and heart failure (Shah *et al.*, 2013). Due to implementation of a wide range of industrial emissions controls and fuel consumption policies, primary fine particle (PM$_{2.5}$, particles with aerodynamic diameter < 2.5 μm) releases and precursors of secondary inorganic aerosol species (sulfur dioxide and nitrogen oxides) were reduced up to 75% in the U.S. (U.S. EPA, 2017a). As a result, ambient PM$_{2.5}$ levels also declined, albeit at slower rate due to non-linear responses in atmospheric chemistry and biomass burning emissions (Chalbot *et al.*, 2013; Squizzato *et al.*, 2018a; Zhang *et al.*, 2018; Blanchard *et al.*, 2019, 2021).
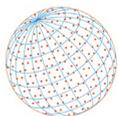
Biomass burning includes wildland fires, agricultural fires, prescribed fires and anthropogenic bioenergy usage (wood burning, use of heating oil, and coal-fired power plant for producing electricity) and it is predominantly comprised of carbonaceous aerosol (i.e., organic carbon (OC) and elemental carbon (EC)) (Lee and Chan, 2015; Masiol et al., 2017a; Squizzato et al., 2018a). The seasonal pattern is frequently an indicator of biomass burning sources with domestic heating including wood burning in the cold months and fires in the warm period (Zhang et al., 2014). There has been a rapid increase in the frequency and intensity of large wildfires that has been linked to the longer and drier summer seasons (McClure and Jaffe, 2018). This increase was associated with higher temperatures during the warmer months, earlier snowmelt, and moisture deficits (Miller and Safford, 2012). Wildfires have been observed to steadily rise from 1984 to 2011 at a rate of 0.6–1.0 annually in the Northern Rockies and Pacific Northwest regions of the U.S. (Dennison et al., 2014). Climate change accounted for 50–60% of the larger wildfires from 1970 to 2016 in Northern Rockies (Westerling, 2016) and has doubled the cumulative wildfire areas burned from 1984 to 2015 in the western U.S. (Abatzoglou and Williams, 2016; Harvey, 2016). Emissions from wildfires have been consistently shown to contribute to ambient $PM_{2.5}$ levels in downwind urban metropolitan areas far away from the fires (Lall and Thurston, 2006; Jaffe et al., 2008; Chalbot et al., 2013; Blanchard et al., 2019; Masiol et al., 2019).

For the New York/New Jersey metropolitan statistical area (MSA), the most populous in the U.S., the 2020 $PM_{2.5}$ weighted annual average and 24-hr concentrations were 8.5 µg m^{-3} and 21 µg m^{-3}, both being below the federal national ambient air quality standards (NAAQS). The 2020 8-hr max ozone (O_3) concentration was 73 ppbv (above the federal NAAQS). Secondary sulfate and nitrate, motor vehicle emissions, road dust, sea salt, and oil combustion were previously identified as the predominant $PM_{2.5}$ sources (Ito et al., 2004; Li et al., 2004). More recently, biomass burning has also been recognized in the region (Blanchard et al., 2019; Masiol et al., 2017a, 2017b, 2019). The latter was associated with increasing OC levels from upwind areas (Blanchard et al., 2019, 2021; Chen et al., 2022).

The objectives for this study were: (i) to identify and quanitify the contributions of $PM_{2.5}$ sources across the NY/NJ MSA; (ii) to estimate the annual trends of $PM_{2.5}$ sources and (iii) to assess the role of anthropogenic and biomass burning emissions. The $PM_{2.5}$ chemical speciation data in four sites during the 2007–2017 period were analyzed using factor analysis to apportion $PM_{2.5}$ sources. Understanding the temporal trends of $PM_{2.5}$ sources is essential to evaluate the efficacy of air pollution controls on industrial and transportation sources over the pase decades. Moreover, the possible contribution of regional and continental wildfires on $PM_{2.5}$ mass and chemical content was assessed.

2 METHODS

2.1 Sampling Sites

The concentrations of $PM_{2.5}$ mass and chemical species were retrieved from the U.S. Environmental Protection Agency's Air Data system (U.S. EPA, 2017b) for the NCore site in Queens, New York (Site #1, EPA AIRS ID: 36-081-0124) and three $PM_{2.5}$ chemical speciation network (CSN) sites, Lower Manhattan (Site #2, Division Street, EPA AIR ID: 36-061-0134), Elizabeth New Jersey (NJ) (Site #3, Elizabeth Lab, EPA AIR ID 34-039-0004) and Chester NJ (Site 4, EPA AIR ID 34-027-3001) for the 2007-2017 period. Fig. 1 shows the locations of the four sites within the NY/NJ MSA. Site #1 is at Queens College, near LaGuardia Airport in New York City. Site #2 is on the roof of Public School 124 in Lower Manhattan. Site #3 is at the intersection of interstate highways I-95 and I-278, near many industrial facilities including oil refineries. Site #4 is on the Department of Public Works building at Chester town in Morris County, NJ. The sites in Queens, Division Street and Elizabeth Lab are in heavily populated areas (more than 3,000,000 residents within 8 km). Chester, a smaller town, is in western NJ, upwind of the New York City metropolitan area.

Daily measurements of $PM_{2.5}$ mass, organic carbon (OC) and elemental carbon (EC), ions (sulfate (SO_4^{2-}), nitrate (NO_3^-), ammonium (NH_4^+), potassium (K^+) and sodium (Na^+) were measured in 1 every 3 days frequency in Sites #1, 2, 3 and 1 every 6 days in Site #4. $PM_{2.5}$ particles collected on polytetrafluoroethylene membrane filters (PTFE) using the MetOne SASS/SuperSASS sampler were analysed gravimetrically for $PM_{2.5}$ mass and by X-ray fluorescence spectrophotometer
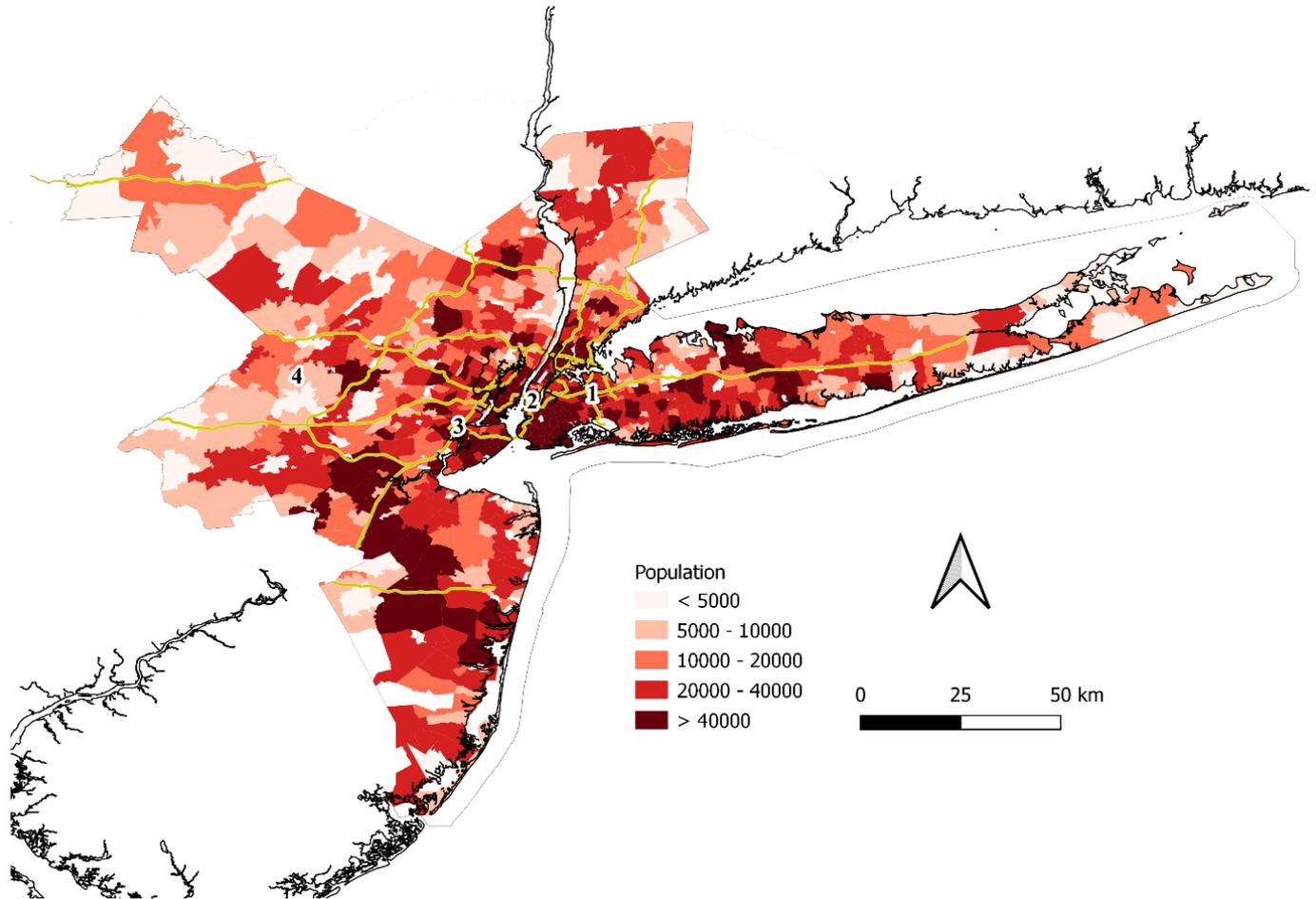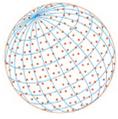
Fig. 1. The PM$_{2.5}$ chemical speciation sites, population, and major road network in NY/NJ MSA.

(PANalytical Epsilon 5 analyzer). Elemental and organic carbon were measured by the thermal optical reflectance (TOR) (Sunset analyzer) for PM$_{2.5}$ collected on quartz fiber filters using the URG 3000N sampler. Water-soluble PM$_{2.5}$ ions were measured by ion chromatography (Dionex ICS-2000, ICS-3000 and Aquion systems) of nylon filters using MetOne SASS/SuperSASS sampler. The U.S. EPA laboratory standard operating protocols and QA/QC protocols are described elsewhere (U.S. EPA, 2019).

2.2 Aerosol Types and Source Apportionment

The major aerosol species (inorganic secondary SO$_4^{2-}$, NO$_3^-$ and NH$_4^+$), organic mass (OM), elemental carbon (EC) and soil dust concentrations were analyzed using the Interagency Monitoring of Protected Visual Environments (IMPROVE) PM$_{2.5}$ mass reconstruction scheme (Malm *et al.*, 2004) according to Eqs. (1)–(4).

$$PM_{2.5} = [EC] + [OM] + [inorganic\ secondary] + [Soil\ dust] \tag{1}$$

$$[OM] = 1.6 \cdot [OC] \tag{2}$$

$$[Inorganic\ Secondary] = 1.29 \cdot [NO_3^-] + 0.944 \cdot [NH_4^+] + 1.02 \cdot [SO]_4^{2-}] \tag{3}$$

$$[Soil\ dust] = 2.2 \cdot [Al] + 2.49 \cdot [Si] + 1.63 \cdot [Ca] + 2.42 \cdot [Fe] + 1.94 \cdot [Ti] \tag{4}$$

where [EC], [OC], [NO$_3^-$], [NH$_4^+$], [SO$_4^{2-}$], [Al], [Si], [Ca], [Fe] and [Ti] were the elemental carbon, organic carbon, nitrate, ammonium, sulfate, aluminum, silica, calcium, iron and titanium concentrations
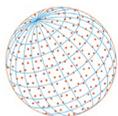
(in µg m^{-3}), respectively. The OC/OM factor of 1.6 was used for urban PM$_{2.5}$ aerosol (Turpin and Lim, 2001). Soil dust was estimated as the sum of the crystal elements as oxides. Discrepancies between measured and reconstructed particle mass may be associated with organic aerosol with a higher OC/OM factor, that is typical of oxygenated and polyfunctional organic compounds in biomass burning aerosol (Kavouras *et al.,* 2012). Sea salt is also not considered in the IMPROVE PM$_{2.5}$ mass reconstruction scheme, which may be important in remote marine environments.

The United States Environmental Protection Agency's Positive Matrix Factorization (PMF) model (Version 5.0) was employed (Norris *et al.,* 2014; Hopke, 2015, 2016). Chemical species with more than 50% of measurements above the limit of detection were included. Missing concentrations and uncertainties were substituted by the geometric mean of the measured concentrations and, four times the geometric mean of measured uncertainties, respectively. The concentrations of chemical species were analyzed by a least-squares method imposing a non-negative restriction on factor (i.e., source) contributions (G(nxp)) and profiles (F(pxm)), during minimization of the objective function (Paatero, 1997). The retained sources were rotated using the F$_{peak}$ variable to reduce ambiguity of the unrotated solution. The best possible number of sources and the rotation was evaluated by a set of statistical tools (Paatero *et al.,* 2005), and by comparison of previously published source profiles. There were up to 990 samples for Sites #1–3 and 660 samples for Site #4. In total, 25 chemical species were used. The S/N ratio varied from 2.27 to 8.49. We ran the model using the robust method for factors varying from 3 to 20 with a random seed and 20 runs per configuration during screening and 100 runs for the final solution. The Q$_{robust}$/Q$_{expected}$ was 1.19. The correlation coefficient varied from 0.25 (for soluble Na$^+$) to 0.95. An eight-factor model with a rotation with F$_{peak}$ = 1.0 was selected. Base and F$_{peak}$ bootstrapping included 200 runs using a minimum R of 0.75 and block size of 6 with random seeding. More than 80% of base and 100% of F$_{peak}$ bootstrapped factors were mapped into the original factors, with no clear pattern for the unmapped factors.

2.3 Statistical Analysis

The non-parametric Mann-Whitney U-test (for two groups) and Kruskal-Wallis (for more than 2 groups) at α = 0.05 was used to test the significant of the difference. The annual trend was computed using the monthly PM$_{2.5}$ source contributions by applying the non-parametric sequential Mann-Kendall test at a confidence level of 95% (Kganyago and Shikwambana, 2020; Shikwambana *et al.,* 2020). Analyses were done using IBM SPSS (Version 27) (IBM Analytics, Armonk, NY).

3 RESULTS AND DISCUSSION

3.1 PM$_{2.5}$ Types and Characteristics

Table 1 shows the PM$_{2.5}$ diagnostic ratios and reconstructed aerosol type concentrations at the four sites. The K/Fe enrichment factor (EF) was computed as the ratio of measured K/Fe to the crystal Soil K/Fe (0.56). The S/SO$_4^{2-}$ mass ratio (from 3.03 to 3.67) and NH$_4^+$/SO$_4^{2-}$ molar ratio

Table 1. PM$_{2.5}$ diagnostic ratios in the NY/NJ MSA during 2007–2017.

Variable	Sampling site			
	Queens College (1)	Division Str. (2)	Elizabeth Lab (3)	Chester (4)
Diagnostic ratio				
SO$_4^{2-}$/total-S	3.11 ± 0.06	3.08 ± 0.09	3.03 ± 0.06	3.67 ± 0.18
NH$_4^+$/SO$_4^{2-}$	2.77 ± 0.10	2.72 ± 0.15	2.56 ± 0.08	2.50 ± 0.13
OC/EC	3.32 ± 0.04	3.30 ± 0.05	2.34 ± 0.04	5.83 ± 0.16
K$^+$/K	0.62 ± 0.01	0.64 ± 0.01	0.58 ± 0.01	0.64 ± 0.01
EF(K/Fe)	1.15 ± 0.02	0.78 ± 0.02	0.80 ± 0.02	2.56 ± 0.05
Aerosol type				
Inorganic species	4.81 ± 0.11	4.99 ± 0.14	4.92 ± 0.14	3.76 ± 0.10
OM	3.51 ± 0.06	4.98 ± 0.07	4.09 ± 0.08	2.71 ± 0.06
EC	0.74 ± 0.01	1.06 ± 0.02	1.28 ± 0.03	0.34 ± 0.01
Soil dust	0.59 ± 0.02	0.61 ± 0.01	0.79 ± 0.03	0.25 ± 0.01
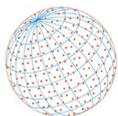
(from 2.50 to 2.77) demonstrated the presence of ammonium sulfate (($NH_4)_2SO_4$) and ammonium bisulfate (($NH_4)HSO_4$) particles (Malm *et al.*, 2002).The OC/EC mass ratio suggested a mixture of combustion sources with a strong fossil fuel signature in urban sites (#1, 2 and 3) (from 2.34–3.32) and biomass in Chester (Site #4, 5.83 ± 0.16). The significant contribution of biomass burning was further corroborated by the increased abundance of soluble potassium (K^+, a tracer of biomass burning) (from 58 to 64% of total K) and the EF(K/Fe) values (from 0.78 to 2.56).

Inorganic species were the predominant $PM_{2.5}$ aerosol components (from 2.76 to 4.99 µg m^{-3}), followed by OM (from 2.71 to 4.98 µg m^{-3}). Inorganic species and OM concentrations accounted for more than 80% of $PM_{2.5}$ mass with a west-to-east spatial gradient from Chester (#4) to Division Street (#2) and slightly decline for Queens College (#1). For EC and soil dust, the highest concentrations were measured at the Elizabeth Lab site (#3), at the intersection of two busy interstate highways. The ratio of the aerosol type concentration measured in urban sites (Queens, Division Str and Elizabeth Lab) as compared to that measured in Chester varied from 1.28–1.38 for inorganic species and 1.30–1.84 for OM, indicating that regional upwind sources may account for most of inorganic species and OM measured at the urban sites. On the other hand, the EC concentration ratio (2.18–3.76) and soil dust (2.36–3.16) indicated the significant contribution of local sources.

3.2 Source Apportionment

The reconstructed $PM_{2.5}$ mass concentrations accounted from 90% at Chester to 106% at Division Street, of measured $PM_{2.5}$ mass (Table 2). Figs. 2 and 3 illustrate the profiles and seasonal contributions of the eight $PM_{2.5}$ sources. The mean contribution of each source of $PM_{2.5}$ mass by site is presented in Table 2. The first factor was assigned to biomass burning with high concentrations of OC, EC, S and SO_4^{2-} (Fig. 2). The OC/EC ratio (4.92 ± 0.10) was indicative of contemporary biomass burning (Turpin and Lim, 2001). The SO_4^{2-}/S ratio (2.57 ± 0.13) was characteristic of a mixture of fresh and aged aerosol (Malm *et al.*, 2002). Biomass burning contributed from 2.9 ± 0.1 µg m^{-3} at Queens College to 3.5 ± 0.1 µg m^{-3} at Elizabeth Lab (Table 2) with slightly higher contributions in summer and winter as compared to fall and spring (Fig. 3). Biomass burning accounted for about 37% of $PM_{2.5}$ in urban sites and 55% of $PM_{2.5}$ mass in Chester. The seasonal trend suggested the influence of local residential wood burning and regional wildland fires (Chalbot *et al.*, 2013).

The second factor was assigned to secondary NO_3^- (in the form of NH_4NO_3) with high concentrations of NO_3^-, NH_4^+, OC, EC, K^+, K and SO_4^{2-} (Fig. 2). The contribution of secondary NO_3^- particles varied from 0.4 ± 0.1 µg m^{-3} in Chester to 0.7 ± 0.1 µg m^{-3} in Queens (from 6% to 8% of $PM_{2.5}$ mass) with the highest contributions during winter and the lowest during summer (Fig. 3). This was consistent with the favorable conditions for gas-to-particles conversion of HNO_3 in low ambient temperatures. The third factor was attributed to diesel combustions because of the high Ni, V, EC, NO_3^-, NH_4^+, SO_4^{2-} and to a lesser extent to Fe and Mn concentrations (Chalbot *et al.*, 2013). The presence of NO_3^- and SO_4^{2-} indicated the contribution from both industrial activities and transportation diesel engines. It accounted for less than 0.1 µg m^{-3} of $PM_{2.5}$ mass in Chester, up to 0.7 ± 0.1 µg m^{-3} in Queens (Table 2) (from 5% to 8% of $PM_{2.5}$ mass in Queens and Division Str. and less than 2% in Elizabeth Lab and Chester) with higher concentrations in the winter (Fig. 3).

Table 2. The mean (± standard error) contributions of sources to $PM_{2.5}$ mass in the NY/NJ MSA during 2007–2017.

| Source	Sampling site			
	Queens College (1)	Division Str. (2)	Elizabeth Lab (3)	Chester (4)
Measured $PM_{2.5}$	8.9 ± 0.2	9.8 ± 0.2	11.1 ± 0.2	7.6 ± 0.2
Estimated $PM_{2.5}$	9.3 ± 0.2	10.4 ± 0.2	11.0 ± 0.3	6.9 ± 0.1
Biomass burning	2.85 ± 0.08	3.27 ± 0.09	3.46 ± 0.11	2.92 ± 0.08
Secondary nitrate	0.66 ± 0.03	0.55 ± 0.03	0.62 ± 0.05	0.37 ± 0.03
Diesel exhausts	0.60 ± 0.04	0.48 ± 0.03	0.22 ± 0.02	0.07 ± 0.01
Road dust	0.27 ± 0.01	0.22 ± 0.01	0.40 ± 0.04	0.12 ± 0.01
Marine emissions	0.07 ± 0.01	0.05 ± 0.01	0.05 ± 0.01	0.01 ± 0.01
Secondary sulfate	1.87 ± 0.12	2.15 ± 0.15	2.43 ± 0.23	1.50 ± 0.08
Traffic exhausts	1.36 ± 0.04	2.06 ± 0.05	2.19 ± 0.07	0.24 ± 0.02
Industrial sources	< 0.1	< 0.1	< 0.1	< 0.1
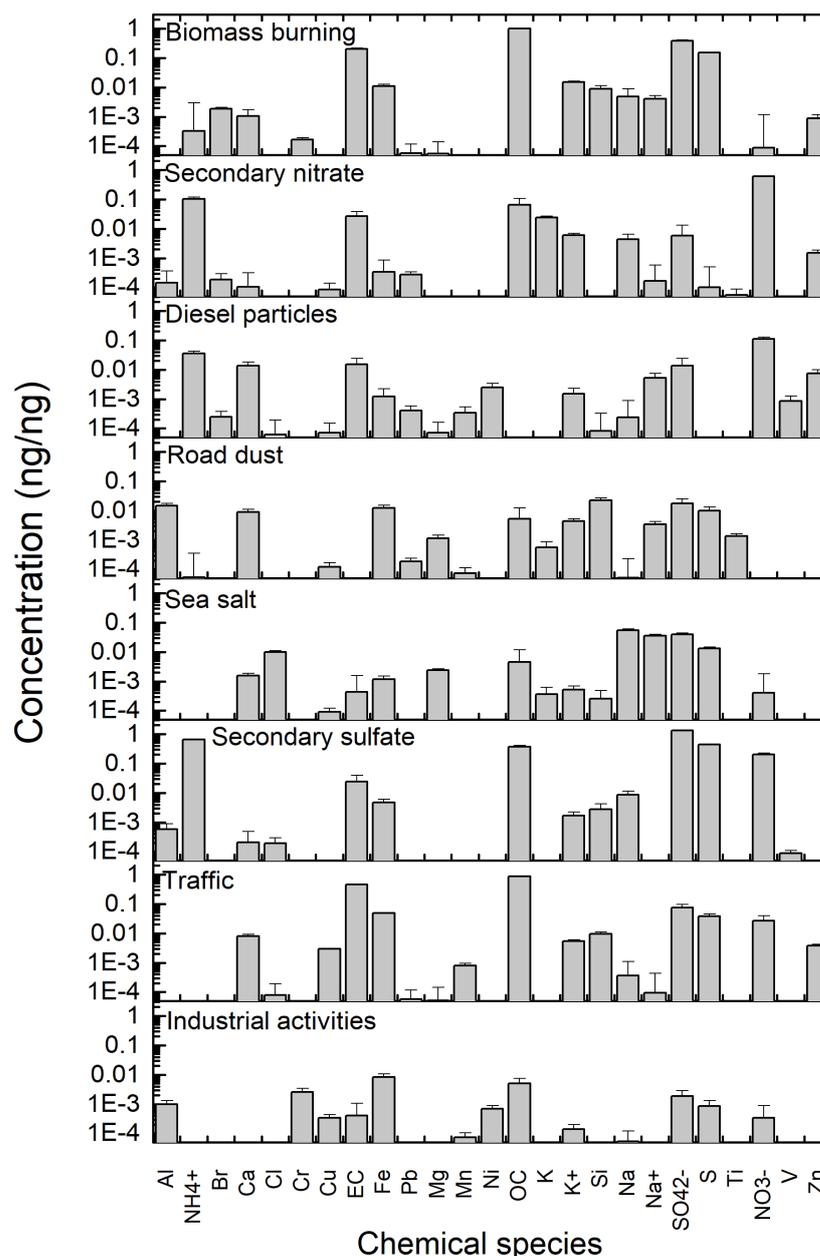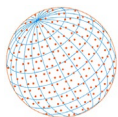
Fig. 2. Profiles of PM$_{2.5}$ sources in the NY/NJ MSA during 2007–2017.

The high concentrations of crystal Al, Si, Ca, Fe and Ti on the fourth factor indicated the presence of soil particles. The components OC, EC, SO$_4^{2-}$, S and Mg hinted at the mechanical resuspension of contaminated road dust (Fig. 2). Mineral and road dust accounted from 0.1 ± 0.1 µg m^{-3} in Chester to 0.4 ± 0.1 µg m^{-3} (from 2% to 4% of PM$_{2.5}$ mass). The highest contributions were computed in spring and summer due to accumulation during the winter of dust and debris deposited in curbs and road shoulders available for resuspension by traffic and patterns of regional dust transport (Fig. 3) (Chalbot *et al.*, 2013). Sea salt particles are correlated with Na, Na$^+$ and Cl in the sixth factor. It also exhibited high contributions from S, SO$_4^{2-}$ and, to a lesser extent, NO$_3^-$ and OC, indicating the possible contribution of harbor and shipping emissions. This was further supported by the SO$_4^{2-}$/S ratio (3.00 ± 0.36) and lack of NH$_4^+$, indicating free H$_2$SO$_4$. The New York port is the destination of container ships (37%), oil/chemical tankers (9%), passenger cruise ships (7%), vehicles carriers (6%) and crude oil tanker (5%). It contributed, on average, less than 0.1 µg m^{-3} on PM$_{2.5}$ mass concentration (less and 1%) across all four sites. Slightly higher contributions were computed in spring than those measured in winter and summer (Fig. 3).
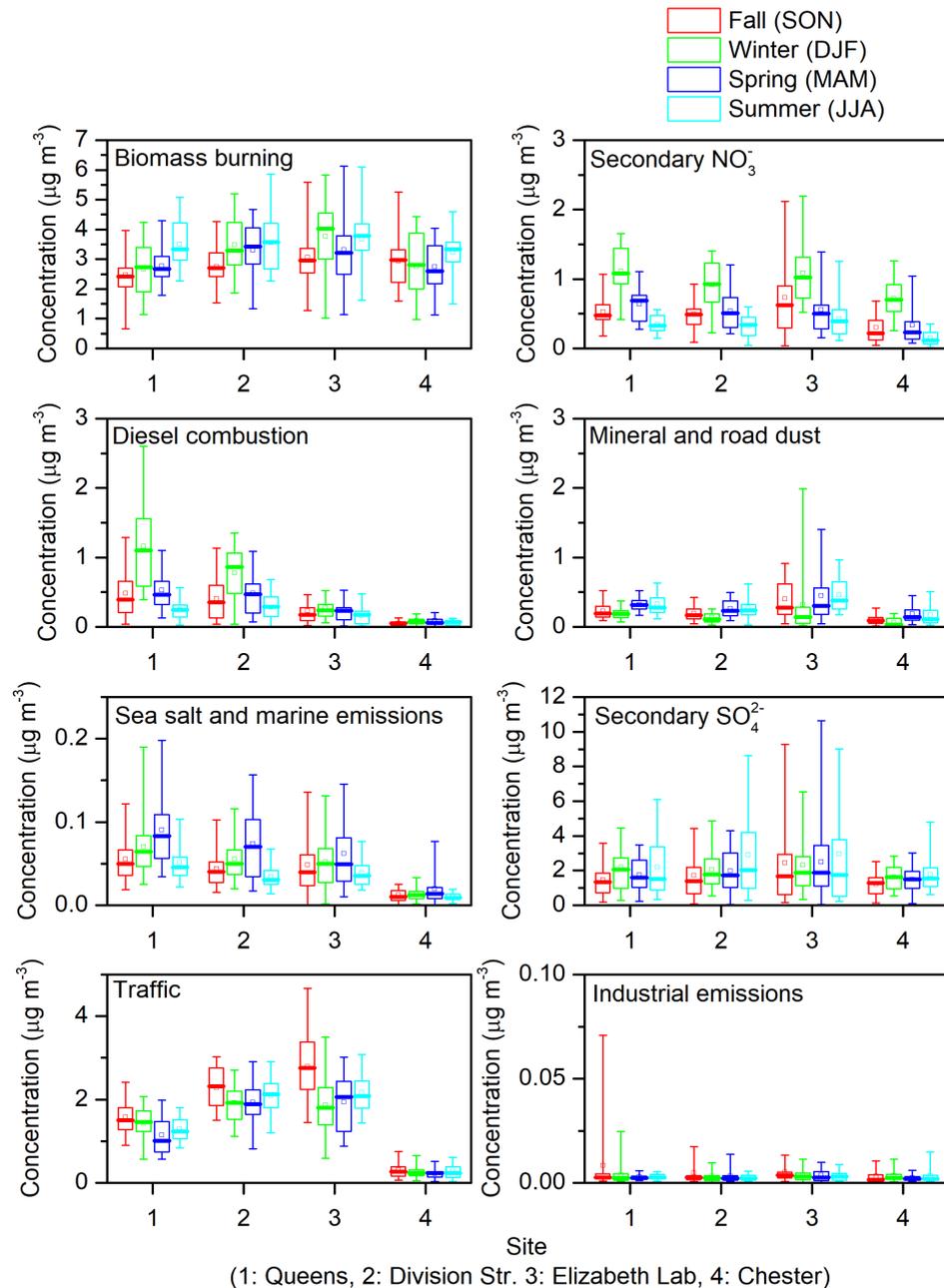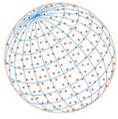
Fig. 3. Seasonal contributions of PM$_{2.5}$ sources in the NY/NJ MSA during 2007–2017.

The sixth factor was attributed to secondary SO$_4^{2-}$ because of the high levels of S, SO$_4^{2-}$, NH$_4^+$ and to a lesser extent of EC and OC. This was further supported by the SO$_4^{2-}$/S ratio (3.02 ± 0.09). This source accounted for 1.5 ± 0.1 µg m^{-3} of PM$_{2.5}$ in Chester to 2.4 ± 0.1 µg m^{-3} of PM$_{2.5}$ in Elizabeth Lab (from 24% to 28%), with the highest contributions being measured in the summer (Fig. 3). Traffic exhausts were identified due to OC, EC, S, SO$_4^{2-}$, NO$_3^-$, Zn and Fe high concentrations in the seventh factor. The low OC/EC ratio (1.84 ± 0.07) was comparable to those computed for urban aerosol and traffic exhausts (Turpin and Lim, 2001). Traffic added 1.5 ± 0.1 µg m^{-3} of PM$_{2.5}$ in Chester up to 2.2 ± 0.1 µg m^{-3} of PM$_{2.5}$ in Elizabeth Lab (Table 2) (17–23%) with slightly higher contribution in the fall at Elizabeth Lab and Division Street and no seasonal variation at Queens and Chester (Fig. 3). Lastly, ferrous, and chrome-related industrial emissions were identified because of the concentrations of heavy metals (Cr, Fe, Ni, Cu). This source contributed minimally (less than 0.1 µg m^{-3} of PM$_{2.5}$; less than 1%) throughout the year (Table 2).
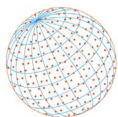
Table 3. The mean (± standard error) annual trend of $PM_{2.5}$ sources in the NY/NJ MSA during 2007–2017.

	Queens College (1)	Division Str (2)	Elizabeth Lab (3)	Chester (4)
$PM_{2.5}$ Mass	−0.42 ± 0.04	−0.54 ± 0.05	−0.36 ± 0.03	−0.23 ± 0.02
Biomass burning	0.07 ± 0.01	−0.04 ± 0.01 (0.22)	−0.12 ± 0.01	0.06 ± 0.01 (0.05)
Secondary nitrate	−0.03 ± 0.01	0.01 ± 0.01 (0.25)	0.02 ± 0.01 (0.1)	0.01 ± 0.01 (0.1)
Diesel exhausts	−0.06 ± 0.01	−0.06 ± 0.01	−0.02 ± 0.01	< 0.01 (0.17)
Road dust	< 0.01 (0.34)	0.01 ± 0.01	0.04 ± 0.01	0.01 ± 00.01
Marine emissions	< 0.01 (0.21)	< 0.01 (0.29)	< 0.01 (0.2)	< 0.01 (0.51)
Secondary sulfate	−0.32 ± 0.03	−0.36 ± 0.03	−0.34 ± 0.03	−0.19 ± 0.02
Traffic exhausts	−0.04 ± 0.01	0.04 ± 0 (0.02)	0.05 ± 0.01 (0.01)	−0.01 ± 0.01 (0.01)
Industrial sources	< 0.01 (0.51)	< 0.01 (0.90)	< 0.01 (0.36)	< 0.01 (0.19)

3.3 Annual Trends

The annual trends of $PM_{2.5}$ mass and source contributions are presented in Table 3. The p-value of the trend analysis is shown in parentheses if $p > 0.001$. $PM_{2.5}$ mass declined by 0.23 ± 0.02 µg m^{-3} yr^{-1} in Chester to 0.54 ± 0.05 µg m^{-3} yr^{-1} in Division Str ($p < 0.001$) This was mostly due to the significant decrease of secondary SO_4^{2-} (from −0.19 ± 0.02 µg m^{-3} yr^{-1} in Chester to −0.36 ± 0.03 µg m^{-3} yr^{-1} in Division Str ($p < 0.001$). The declining trends among all four sites were indicative of the regional SO_4^{2-} origins from power plants (Emami *et al.*, 2018). The annual SO_4^{2-} concentration in the NY/NJ MSA dropped by 77.5%, from 3.8 µg m^{-3} in 2007 to 0.9 µg m^{-3} in 2017. This was comparable to national SO_2 reductions (78.2%, from 11.7 × 10^6 tons in 2007 to 1.9 × 10^6 tons in 2017) (U.S. EPA, 2017a).

For locally important sources such as secondary nitrate, traffic exhausts and diesel emissions, site-specific annual trends were observed. More specifically, secondary NO_3^- and primary traffic-related gasoline exhausts declined in Queens (−0.19 ± 0.02 µg m^{-3} yr^{-1} for secondary NO_3^- and −0.04 ± 0.01 µg m^{-3} yr^{-1} for traffic exhausts, $p < 0.001$) but slightly increased in the remaining sites, albeit without statistically insignificance (Table 3) The NO_3^- annual concentrations declined, from 1.7 µg m^{-3} in 2007 to 1.0 µg m^{-3} in 2017 was consistent with the national NO_x emission reduction (45.6%) (U.S. EPA, 2017a). The good agreement between reductions of secondary SO_4^{2-} and NO_3^- and their precursors emissions (SO_2 and NO_x), despite that NH_3 emissions remained relatively unchanged nationally, further confirmed strong regional contributions and the negligible influence of local NH_3 emissions. For diesel exhausts, contributions decreased in the three urban sites, from −0.02 ± 0.01 µg m^{-3} yr^{-1} in Elizabeth Lab to −0.06 ± 0.01 µg m^{-3} yr^{-1} in Queens and Division Str. The annual trend of mineral and road dust was comparable to that of traffic exhausts, with an increasing trend in Division Str (0.01 ± 0.01 µg m^{-3} yr^{-1}) and Elizabeth Lab (0.04 ± 0.01 µg m^{-3} yr^{-1}) and minimal changes in Queens and Chester. No significant trends were computed for contaminated sea salt and industrial emissions.

Biomass burning contributions declined substantially in Elizabeth Lab (−0.12 ± 0.01 µg m^{-3} yr^{-1}, $p < 0.001$) and Division Str (−0.04 ± 0.01 µg m^{-3} yr^{-1}, $p = 0.22$) but increased in Chester (slightly, 0.01 ± 0.01 µg m^{-3} yr^{-1}, $p = 0.1$) and Queens (0.07 ± 0.01 µg m^{-3} yr^{-1}, $p < 0.001$). The inconsistent annual trends may be influenced by climatology and local domestic emissions (Rattigan *et al.*, 2016; Squizzato *et al.*, 2018b; Pitiranggon *et al.*, 2021). Wood burning for heating and recreational reasons is allowed in both New York and New Jersey; however due to the type of residential units, its prevalence may be higher in communities with single house units (e.g., Chester and Queens) as compared to building apartments (e.g., Division Str). The site in Elizabeth Lab is in an industrial area.

3.4 Biomass Burning Sources

Fig. 4 illustrates the annual trends of biomass burning in summer (May–September) and winter (November to March), the number and area burnt (in acres) by lightning ignited wildland fires in the U.S. (data obtained from the National Interagency Fire Center) and the monthly minimum temperature and number of days with temperature less than 0°C in New York City (New York City Central Park; NOAA NCDC site: USW00094728) during the 2007–2017 period. Since 2010, there appears to be a temporal correlation of the number of wildfires naturally induced by lightning and, to a lesser extent, the area burnt and summertime biomass burning contributions. Wildfires
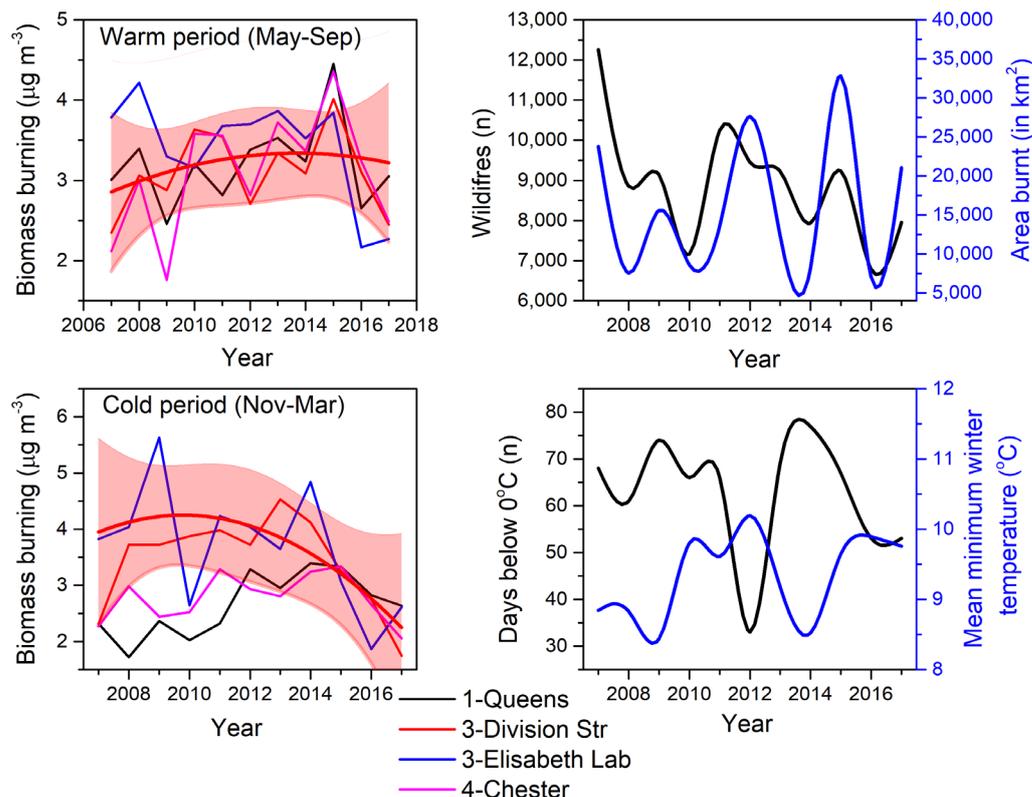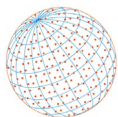
Fig. 4. Annual trend of biomass burning contributions in summer (May–September) and winter (November–March), number and area burnt by wildfires and, minimum winter temperatures and number of days with temperature less than 0°C.

burned more than 15,000 km^2 per year in the U.S. in 2007–2009, as compared to 17,000 km^2 during the 2011–2013 period and over 20,000 km^2 during the 2015–2017 period. We have previously shown that changes in the El-Nino southern oscillation were correlated with wildfires in Eastern United States and episodes of smoke-related high ozone pollution (Singh and Kavouras, 2022). Higher wintertime biomass burning contributions prior to 2010 and in 2014 were associated with colder winters with an average minimum temperature of less than 9°C and prolonged periods of extreme cold more than 60 days. On the other hand, local biomass burning contributions declined when the average minimum temperature was above 0°C and the number of cold days declined.

4 CONCLUSIONS

The sources of fine particles in the NY/NJ MSA for the 2007–2017 period were biomass burning (37–55%), secondary sulfate (24–28%), primary traffic emissions (17–23%), secondary nitrate (6–8%), diesel emissions (1–8%), road dust (2–4%), sea salt (< 1%), and industrial emissions (< 1%). The seasonality of secondary NO_3^-, secondary SO_4^{2-} and dust was consistent with those previously observed in urban environments and the effect of local meteorology and emissions. PM$_{2.5}$ mass concentrations declined by 0.23–0.54 µg m^{-3} yr^{-1}. Secondary NO_3^- and secondary SO_4^{2-} declines were consistent with the reductions on NO$_x$ and SO$_2$ emission from mobile and point sources, respectively. The seasonal variability of biomass burning to PM$_{2.5}$ mass was indicative of local wood burning for domestic heating and recreational activities and regional smoke from wildfires contributed to PM$_{2.5}$ in winter and summer, respectively. Wintertime biomass burning appeared to be related to the number of cold days and average minimum temperature in the region. The number and area burnt by wildfires was also associated with the interannual variability of biomass burning contribution in the summer. The findings of this study show that changes in
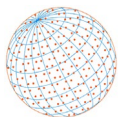
PM$_{2.5}$ mass concentrations in the NY/NJ MSA are responding to reductions of secondary sulfate and nitrate precursors from anthropogenic sources. As a result, biomass burning is the predominant PM$_{2.5}$ source. Its contributions appear to be related to local and regional climatology affecting the frequency and intensity of cold weather in the winter and wildfires in the summer.

ACKNOWLEDGMENTS

DISCLAIMER

The authors declare no potential conflicts of interest.

REFERENCES

Abatzoglou, J.T., Williams, A.P. (2016). Impact of anthropogenic climate change on wildfire across western US forests. PNAS 113, 11770–11775. https://doi.org/10.1073/pnas.1607171113

Blanchard, C.L., Shaw, S.L., Edgerton, E.S., Schwab, J.J. (2019). Emission influences on air pollutant concentrations in New York state: II. PM$_{2.5}$ organic and elemental carbon constituents. Atmos. Environ.: X 3, 100039. https://doi.org/10.1016/j.aeaoa.2019.100039

Blanchard, C.L., Shaw, S.L., Edgerton, E.S., Schwab, J.J. (2021). Ambient PM$_{2.5}$ organic and elemental carbon in New York City: Changing source contributions during a decade of large emission reductions. J. Air Waste Manage. Assoc. 71, 995–1012. https://doi.org/10.1080/10962247.2021.1914773

Chalbot, M.C., McElroy, B., Kavouras, I. (2013). Sources, trends and regional impacts of fine particulate matter in southern Mississippi Valley: significance of emissions from sources in the Gulf of Mexico coast. Atmos. Chem. Phys. 13, 3721–3732. https://doi.org/10.5194/acp-13-3721-2013

Chen, Y., Rich, D.Q., Hopke, P.K. (2022). Long-term PM$_{2.5}$ source analyses in New York City from the perspective of dispersion normalized PMF. Atmos. Environ. 272, 118949. https://doi.org/10.1016/j.atmosenv.2022.118949

Dennison, P.E., Brewer, S.C., Arnold, J.D., Moritz, M.A. (2014). Large wildfire trends in the western United States, 1984–2011. Geophys. Res. Lett. 41, 2928–2933. https://doi.org/10.1002/2014GL059576

Emami, F., Masiol, M., Hopke, P.K. (2018). Air pollution at Rochester, NY: Long-term trends and multivariate analysis of upwind SO$_2$ source impacts. Sci. Total Environ. 612, 1506–1515. https://doi.org/10.1016/j.scitotenv.2017.09.026

Evans, K.A., Hopke, P.K., Utell, M.J., Kane, C., Thurston, S.W., Ling, F.S., Chalupa, D., Rich, D.Q. (2017). Triggering of ST-elevation myocardial infarction by ambient wood smoke and other particulate and gaseous pollutants. J. Exposure Sci. Environ. Epidemiol. 27, 198–206. https://doi.org/10.1038/jes.2016.15

Harvey, B.J. (2016). Human-caused climate change is now a key driver of forest fire activity in the western United States. Proc. Natl. Acad. Sci. U.S.A. 113, 11649–11650. https://doi.org/10.1073/pnas.1612926113

Hopke, P.K. (2015). Applying Multivariate Curve Resolution to Source Apportionment of the Atmospheric Aerosol, in: 40 Years of Chemometrics – From Bruce Kowalski to the Future, American Chemical Society, pp. 129–157. https://doi.org/10.1021/bk-2015-1199.ch006

Hopke, P.K. (2016). Review of receptor modeling methods for source apportionment. J. Air Waste Manage. Assoc. 66, 237–259. https://doi.org/10.1080/10962247.2016.1140693

Ito, K., Xue, N., Thurston, G. (2004). Spatial variation of PM$_{2.5}$ chemical species and source-apportioned mass concentrations in New York City. Atmos. Environ. 38, 5269–5282. https://doi.org/10.1016/j.atmosenv.2004.02.063

Jaffe, D., Hafner, W., Chand, D., Westerling, A., Spracklen, D. (2008). Interannual variations in PM$_{2.5}$ due to wildfires in the western United States. Environ. Sci. Technol. 42, 2812–2818. https://doi.org/10.1021/es702755v
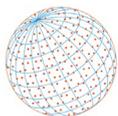
Kavouras, I.G., Nikolich, G., Etyemezian, V., DuBois, D.W., King, J., Shafer, D. (2012). In situ observations of soil minerals and organic matter in the early phases of prescribed fires. J. Geophys. Res. 117, D12310. https://doi.org/10.1029/2011JD017420

Kganyago, M., Shikwambana, L. (2020). Assessment of the characteristics of recent major wildfires in the USA, Australia and Brazil in 2018–2019 using multi-source satellite products. Remote Sens. 12, 1803. https://doi.org/10.3390/rs12111803

Lall, R., Thurston, G.D. (2006). Identifying and quantifying transported vs. local sources of New York City $PM_{2.5}$ fine particulate matter air pollution. Atmos. Environ. 40, 333–346. https://doi.org/10.1016/j.atmosenv.2006.04.068

Lee, W.W., Chan, W.T. (2015). Calibration of single-particle inductively coupled plasma-mass spectrometry (SP-ICP-MS). J. Anal. At. Spectrom. 30, 1245–1254. https://doi.org/10.1039/C4JA00408F

Li, Z., Hopke, P.K., Husain, L., Qureshi, S., Dutkiewicz, V.A., Schwab, J.J., Drewnick, F., Demerjian, K.L. (2004). Sources of fine particle composition in New York City. Atmos. Environ. 38, 6521–6529. https://doi.org/10.1016/j.atmosenv.2004.08.040

Link, M.S., Luttmann-Gibson, H., Schwartz, J., Mittleman, M.A., Wessler, B., Gold, D.R., Dockery, D.W., Laden, F. (2013). Acute exposure to air pollution triggers atrial fibrillation. J. Am. Coll. Cardiol. 62, 816–825. https://doi.org/10.1016/j.jacc.2013.05.043

Malm, W.C., Schichtel, B.A., Ames, R.B., Gebhart, K.A. (2002). A 10-year spatial and temporal trend of sulfate across the United States. J. Geophys. Res. 107, 4627. https://doi.org/10.1029/2002JD002107

Malm, W.C., Schichtel, B.A., Pitchford, M.L., Ashbaugh, L.L., Eldred, R.A. (2004). Spatial and monthly trends in speciated fine particle concentration in the United States. J. Geophys. Res. 109, D03306 https://doi.org/10.1029/2003JD003739

Masiol, M., Hopke, P., Felton, H., Frank, B., Rattigan, O., Wurth, M., LaDuke, G. (2017a). Analysis of major air pollutants and submicron particles in New York City and Long Island. Atmos. Environ. 148, 203–214. https://doi.org/10.1016/j.atmosenv.2016.10.043

Masiol, M., Hopke, P., Felton, H., Frank, B., Rattigan, O., Wurth, M., LaDuke, G. (2017b). Source apportionment of $PM_{2.5}$ chemically speciated mass and particle number concentrations in New York City. Atmos. Environ. 148, 215–229. https://doi.org/10.1016/j.atmosenv.2016.10.044

Masiol, M., Squizzato, S., Rich, D.Q., Hopke, P.K. (2019). Long-term trends (2005–2016) of source apportioned $PM_{2.5}$ across New York State. Atmos. Environ. 201, 110–120. https://doi.org/10.1016/j.atmosenv.2018.12.038

McClure, C.D., Jaffe, D.A. (2018). US particulate matter air quality improves except in wildfire-prone areas. PNAS, 115: 7901–7906. https://doi.org/10.1073/pnas.1804353115

Miller, J.D., Safford, H. (2012). Trends in wildfire severity: 1984 to 2010 in the Sierra Nevada, Modoc Plateau, and southern Cascades, California, USA. Fire Ecol. 8, 41–57. https://doi.org/10.4996/fireecology.0803041

Norris, G., Duvall, R., Brown, S., Bai, S. (2014). EPA Positive Matrix Factorization (PMF) 5.0 Fundamentals and User Guide. EPA/600/R-14/108. U.S. Environmental Protection Agency, Washington, DC.

Paatero, P. (1997). Least squares formulation of robust non-negative factor analysis. Chemom. Intell. Lab. Syst., 37, 23–35. https://doi.org/10.1016/S0169-7439(96)00044-5

Paatero, P., Hopke, P.K., Begum, B.A., Biswas, S.K. (2005). A graphical diagnostic method for assessing the rotation in factor analytical models of atmospheric pollution. Atmos. Environ. 39, 193–201. https://doi.org/10.1016/j.atmosenv.2004.08.018

Pitiranggon, M., Johnson, S., Haney, J., Eisl, H., Ito, K. (2021). Long-term trends in local and transported $PM_{2.5}$ pollution in New York City. Atmos. Environ. 248, 118238. https://doi.org/10.1016/j.atmosenv.2021.118238

Rajagopalan, S., Al-Kindi, S.G., Brook, R.D. (2018). Air pollution and cardiovascular disease. J. Am. Coll. Cardiol. 72, 2054–2070. https://doi.org/10.1016/j.jacc.2018.07.099

Rattigan, O.V., Civerolo, K.L., Felton, H.D., Schwab, J.J., Demerjian, K.L. (2016). Long term trends in New York: $PM_{2.5}$ mass and particle components. Aerosol Air Qual. Res. 16, 1191–1205. https://doi.org/10.4209/aaqr.2015.05.0319

Shah, A.S., Langrish, J.P., Nair, H., McAllister, D.A., Hunter, A.L., Donaldson, K., Newby, D.E., Mills, N.L. (2013). Global association of air pollution and heart failure: A systematic review and meta-

analysis. Lancet 382, 1039–1048. https://doi.org/10.1016/S0140-6736(13)60898-3
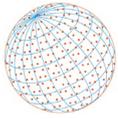
Shah, A.S.V., Lee, K.K., McAllister, D.A., Hunter, A., Nair, H., Whiteley, W., Langrish, J.P., Newby, D.E., Mills, N.L. (2015). Short term exposure to air pollution and stroke: Systematic review and meta-analysis. BMJ 350, h1295. https://doi.org/10.1136/bmj.h1295

Shikwambana, L., Mhangara, P., Mbatha, N. (2020). Trend analysis and first time observations of sulphur dioxide and nitrogen dioxide in South Africa using TROPOMI/Sentinel-5 P data. Int. J. Appl. Earth Obs. Geoinf. 91, 102130. https://doi.org/10.1016/j.jag.2020.102130

Singh, S., Kavouras, I.G. (2022). Trends of ground-level ozone in New York city area during 2007–2017. Atmosphere 13, 114. https://doi.org/10.3390/atmos13010114

Squizzato, S., Masiol, M., Rich, D.Q., Hopke, P.K. (2018a). PM$_{2.5}$ and gaseous pollutants in New York State during 2005–2016: Spatial variability, temporal trends, and economic influences. Atmos. Environ. 183, 209–224. https://doi.org/10.1016/j.atmosenv.2018.03.045

Squizzato, S., Masiol, M., Rich, D.Q., Hopke, P.K. (2018b). A long-term source apportionment of PM$_{2.5}$ in New York State during 2005–2016. Atmos. Environ. 192, 35–47. https://doi.org/10.1016/j.atmosenv.2018.08.044

Turpin, B.J., Lim, H.J. (2001). Species contributions to PM$_{2.5}$ mass concentrations: Revisiting common assumptions for estimating organic mass. Aerosol. Sci. Technol. 35, 602–610. https://doi.org/10.1080/02786820119445

U.S. Environmental Protection Agency (U.S. EPA) (2017a). Air Emissions Inventories. https://www.epa.gov/air-emissions-inventories/air-pollutant-emissions-trends-data (accessed 1 September 2020).

U.S. Environmental Protection Agency (U.S. EPA) (2017b). Air Data. Pre-Generated Data Files. https://aqs.epa.gov/aqsweb/airdata/download_files.html#Daily (accessed 1 June 2020).

U.S. Environmental Protection Agency (U.S. EPA) (2019). Chemical Speciation Network - Quality Assurance. https://www.epa.gov/amtic/chemical-speciation-network-quality-assurance (accessed 15 May 2022).

Westerling, A.L. (2016). Increasing western US forest wildfire activity: Sensitivity to changes in the timing of spring. Philos. Trans. R. Soc. London, Ser. B 371, 20150178. https://doi.org/10.1098/rstb.2015.0178

Zhang, W., Lin, S., Hopke, P.K., Thurston, S.W., van Wijngaarden, E., Croft, D., Squizzato, S., Masiol, M., Rich, D.Q. (2018). Triggering of cardiovascular hospital admissions by fine particle concentrations in New York state: Before, during, and after implementation of multiple environmental policies and a recession. Environ. Pollut. 242, 1404–1416. https://doi.org/10.1016/j.envpol.2018.08.030

Zhang, X., Kondragunta, S., Roy, D.P. (2014). Interannual variation in biomass burning and fire seasonality derived from geostationary satellite data across the contiguous United States from 1995 to 2011. J. Geophys. Res. 119, 1147–1162. https://doi.org/10.1002/2013JG002518